Synthetic Metals, 29 (1989) F445–F452

ELECTRONIC INTERFERENCE, ELASTICITY, AND SCANNING TUNNELING MICROSCOPY STUDIES OF THE CHARGE DENSITY WAVE CONDUCTOR $K_{0.3}MoO_3$

A. ZETTL[1], L.C. BOURNE[1], J. CLARKE[1,2], M.F. CROMMIE[1], M.F. HUNDLEY[1,*], R.E. THOMPSON[1,2], AND U. WALTER[1,+]

[1]Department of Physics, University of California at Berkeley, Berkeley, California 94720 (U.S.A.)

[2]Center for Advanced Materials, Lawrence Berkeley Laboratory, Berkeley, California 94720 (U.S.A.)

ABSTRACT

Charge density wave (CDW) dynamics and statics are explored in the blue bronze $K_{0.3}MoO_3$. For very thin (optically transparent, d≈0.2μm) platelets highly coherent response obtains, and in the presence of dc electric fields the ac conductivity shows high frequency interference structure. This interference is discussed in terms of a resonant circuit analog. At low temperatures, the zero differential resistance state is associated with dramatic changes in the elastic constants of the crystal. However, the effects of sample core heating may be important. Both above and below the CDW transition temperature, the surface of $K_{0.3}MoO_3$ has been examined by atomic resolution scanning tunneling microscopy. Although the underlying lattice is clearly resolved, no CDW superstructure has been imaged on the crystal surface.

INTRODUCTION

Numerous structural, transport, magnetic resonance, and elastic experiments on the blue bronze $K_{0.3}MoO_3$ have demonstrated the existence of a collective-mode charge density wave (CDW) state below the metal-insulator transition at T_p=180K. Many of the observed properties (such as lattice superstructure, elastic anomalies at T_p, nonlinear and frequency dependent conductivity, narrow- and broad-band noise, etc.) are quite analogous to those observed in other CDW

*Present address: Los Alamos National Laboratory, Los Alamos, New Mexico 87545 (U.S.A.)

+Present address: Lehrstuhl für Angewandte Physik, Universität Köln, Zülpicher Str. 77, 5000 Köln 41 (F.R.G.)

0379-6779/89/$3.50

materials, for example TaS_3 and $NbSe_3$. On the other hand, several features set $K_{0.3}MoO_3$ apart from other CDW conductors. The typical blue bronze crystal displays only weak low frequency interference effects in the presence of ac+dc electric fields, which suggests that high frequency effects are damped out by the domain structure of typically large crystal volumes. Also, in blue bronze no lattice softening is observed upon CDW depinning, in contrast to all other measured CDW materials. Finally, at very low temperatures, the insulating state switches into a zero differential resistance state in which the CDW apparently slides without excess dissipation, suggestive of an "ideal" Fröhlich state. The critical electric field necessary to induce this anomalous conduction is much smaller than that observed for the similar materials TaS_3 and $(TaSe_4)_2I$.

We have performed transport, elastic, and structural studies which relate to the unusual features of $K_{0.3}MoO_3$. First, the complex ac conductivity has been determined in the presence of dc bias fields using samples with limited domain structure. The samples are thin (optically transparent) platelets with well-defined geometry and uniform current distribution. Both low frequency and high frequency interference is observed. The interference is described in terms of a resonant circuit response, and a universal "resonance response phase" is determined. Second, the single crystal Young's modulus and internal friction have been measured in the presumed ideal Fröhlich conducting state at low temperatures (T≈4K). Onset of electrical conduction results in dramatic changes of the elastic constants. Unfortunately, it is difficult to distinguish intrinsic elastic changes from potential sample core heating (which may of course also influence the electrical response). Third, the surface of $K_{0.3}MoO_3$ has been imaged both above and below T_p by atomic resolution scanning tunneling microscopy. High-quality lattice images are obtained, but the CDW superstructure is not observed on the crystal surface.

AC CONDUCTIVITY INTERFERENCE

In typical blue bronze samples (dimensions ~fractions of mm) the response is rather incoherent, as evidenced by a general lack of clean narrow-band noise (NBN) peaks or Shapiro steps interference. It has recently been demonstrated, however, that CDW coherence is dramatically improved in $K_{0.3}MoO_3$ in samples of submicron size[1]. Thin rectangular plates of thickness ~0.1-0.2μm consistently show very sharp NBN peaks and Shapiro step interference. We presently investigate the complex ac conductivity $\sigma(\omega)$ of such thin samples for dc induced interference structure.

Fig. 1a shows the ac dielectric constant $\varepsilon(\omega)=4\pi Im\sigma(\omega)/\omega$ of $K_{0.3}MoO_3$ at T=77K for four values of $\omega/2\pi$. At 1kHz, a dramatic "inductive" dip is observed, consistent with previous studies[2,3] of $NbSe_3$ and $K_{0.3}MoO_3$. This dip is observed in most (typical volume) $K_{0.3}MoO_3$ samples under similar drive

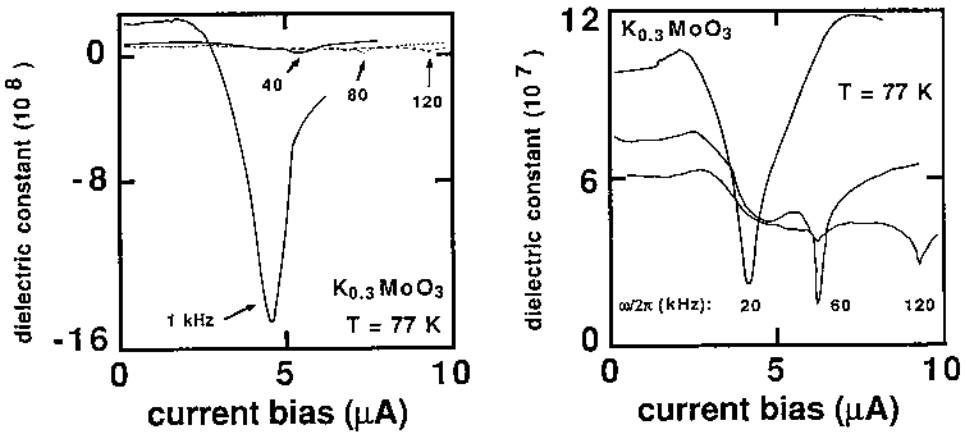

Fig. 1. Bias-dependent dielectric constant in $K_{0.3}MoO_3$. (a) over a large frequency range, and (b) at selected high frequencies.

conditions. The magnitude of the dip decreases and its position moves to higher dc bias as ω increases. For a typical sample, no sharp structure is observed in $\varepsilon(\omega)$ for $\omega/2\pi$ above ~50kHz. For the thin (d=0.2μm) sample of Fig. 1a, on the other hand, small but well-defined anomalies are still observed at 120kHz. The position of the dips marks interference between the NBN and the ac drive at frequency $\omega/2\pi$. Fig. 1b shows high frequency interference dips in $\varepsilon(\omega)$ in greater detail. Subharmonic interference is observed, and even at 120kHz the interference remains sharp. Only at very low frequencies does the inductive dip actually drive ε negative (a similar effect is observed[2] in $NbSe_3$).

Fig. 2 compares anomalies in $\varepsilon(\omega)$ to corresponding structure in $Re\sigma(\omega)$. The

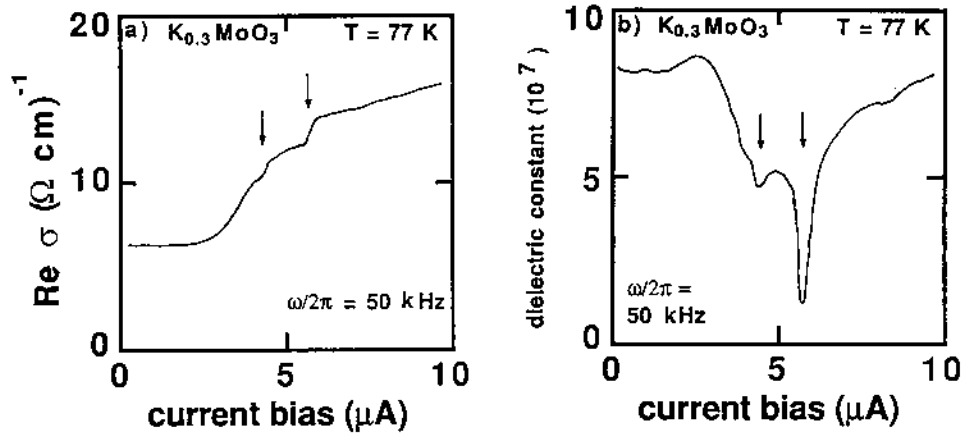

Fig. 2. Complex ac conductivity $\sigma(\omega)$ in $K_{0.3}MoO_3$ as a function of dc bias.

vertical arrows identify those current bias levels which generate NBN frequencies of 25 and 50kHz. Anomalies in $\varepsilon(\omega)$ are associated with anomalies in $Re\sigma(\omega)$.

Fig. 3a shows the interference structure in $Re\sigma(\omega)$ and $Im\sigma(\omega)$ as ω is swept, for fixed bias above threshold (this is in contrast to Figs. 1 and 2 where ω was fixed and bias was swept). Subharmonic and numerous harmonic interference anomalies are observed. Fig. 3b shows in detail the behavior of the fundamental interference.

We now discuss these results. The interference structure manifests itself as sharp inductive-like dips in $Im\sigma(\omega)$ (or equivalently in $\varepsilon(\omega)$) and in $Re\sigma(\omega)$ as gradual positive and negative peaks located equidistant above and below the interference position, respectively. At peak interference (i.e. at the peak of $\varepsilon(\omega)$, which we define as resonance), $Re\sigma(\varepsilon)$ appears unchanged from its inferred value if no interference had occurred. A comparison of the anomalies in $Re\sigma(\omega)$ for bias sweep (Fig. 2) and for frequency sweep (Fig. 3) shows that the ordering of the positive and negative peaks relative to the central resonance position are interchanged in the two cases. This suggests that the resonance is best characterized by

$$\Delta f = f_{NBN} - \omega/2\pi. \qquad (1)$$

The response during interference is functionally analogous to a resonant

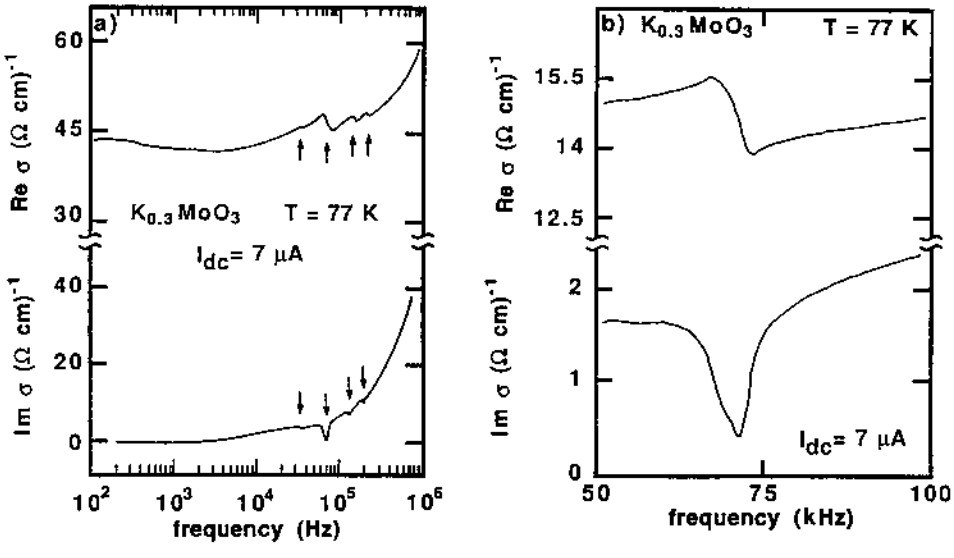

Fig. 3. Complex ac conductivity $\sigma(\omega)$ in $K_{0.3}MoO_3$ as a function of frequency. The dc bias is fixed such that f_{NBN}=70kHz. (b) shows the fundamental resonance with a linear frequency scale.

harmonic oscillator circuit, but with a phase shift which allows the main resonance at $\Delta f=0$ to occur as a negative pointing peak in $Im\sigma(\omega)$. The total sample current response to a drive of the form $V = V_{dc} + V_{ac}\cos(\omega t)$ can be written as

$$I = I_{CDW,dc} + e^{i\omega t}(I_n + I_{CDW,ac}e^{i\theta} + I_{NBN}e^{i\phi}) \qquad (2)$$

where I_n denotes the contribution of normal electrons. The total ac conductivity at the probe frequency is then

$$\sigma(\omega) = \langle I/V \rangle = I_n/V_{ac} + e^{i\theta}I_{CDW,ac}/V_{ac} + e^{i\phi}I_{NBN}\delta_{\omega,\omega(NBN)}/V_{ac} \qquad (3)$$

where δ is a Kronecker delta. For $\omega \neq \omega_{NBN}$, only the normal and CDW conductivities contribute to the response. For $\omega=\omega_{NBN}$, an extra contribution results from the NBN signal. In order for the resonant conductivity enhancement to appear as a negative dip in $Im\sigma$, the phase angle at resonance must be $\phi=-\pi/2$. This defines a universal "resonance response phase". The value $-\pi/2$ agrees with the response phase obtained from pulsed NBN studies[4]. Eq. (3) predicts for the magnitude of the inductive dip

$$\Delta Im\sigma(\omega=\omega_{NBN}) = LI_{NBN}/AV_{ac} \qquad (4)$$

where L and A are sample length and area. Eq. (4) suggests that the dip magnitude depends only on NBN amplitude, and hence to a first approximation $\Delta Im\sigma$ should be independent of ω. Experimentally, this is indeed the case. By a Kramers-Kronig analysis, positive and negative peaks in $Re\sigma(\omega)$ must occur if a sharp, negative resonance peak appears in $Im\sigma(\omega)$. Off (but near) resonance (i.e. $\Delta f \neq 0$) the phase ϕ of the NBN signal relative to the ac probing singal must depart from the resonance value $-\pi/2$. The limiting values are $\phi \rightarrow -\pi$ for $\Delta f << 0$ and $\phi \rightarrow 0$ for $\Delta f >> 0$. Eq. (4) predicts a dip magnitude $\Delta Im\sigma$ consistent with experiment. In addition, from the resonance circuit model it is predicted that the peak sizes in $Re\sigma$ are given by $\Delta Im\sigma/\Delta Re\sigma=2.0$. Fig. 2 suggests for this ratio a value of 1.7; Fig. 3 gives a ratio 1.9.

ELASTIC PROPERTIES OF $K_{0.3}MoO_3$ AT LOW TEMPERATURE

Previous measurements have shown that the elastic properties of $K_{0.3}MoO_3$ are sensitive to CDW formation[5]. Rather remarkably, however, the longitudinal Young's modulus is relatively insensitive to CDW motion at moderate temperatures in the CDW state. This is in contrast to $NbSe_3$ and TaS_3, for example, where both Young's modulus Y and internal friction δ change dramatically upon CDW depinning. At moderate temperatures CDW depinning in $K_{0.3}MoO_3$ has been well

established. Of great current interest is the unusual and extremely abrupt onset of conduction at very low temperatures (~4K)[6]. For moderate applied electric fields, zero differential resistance is observed. This has been interpreted as nearly ideal Fröhlich conduction (no dissipation).

We have investigated the longitudinal Young's modulus and internal friction in $K_{0.3}MoO_3$ in the low temperature pinned and highly-conducting states. The measurements were performed using a modified vibrating reed technique. Fig. 4a shows the I-V (voltage driven) characteristics, Y, and amplitude~$1/\delta$ for $K_{0.3}MoO_3$ at 4.2 K. The sharp onset in electrical conduction is associated with changes in the elastic properties. Fig. 4b shows the onset region in greater detail. Both Y and $1/\delta$ decrease as the conduction increases. Similar effects were observed for samples which showed zero differential resistance, or even unstable regions of negative differential resistance.

The experiments of Fig. 4 were repeated in the presence of superposed rf fields. The rf field (ranging from 100 Hz to 5MHz) decreased the threshold voltage for conductivity and elastic changes, and enhanced the magnitude of the changes in the nonlinear region. No effect in elastic properties of the crystal was observed for an rf signal (sine wave or square wave) of any frequency or amplitude if the sample was biased below threshold (E_{dc}=0 or $0.9E_T$).

It is tempting to associate the elastic changes observed in Fig. 4 with a depinning and subsequent Fröhlich motion of the CDW. However, from our

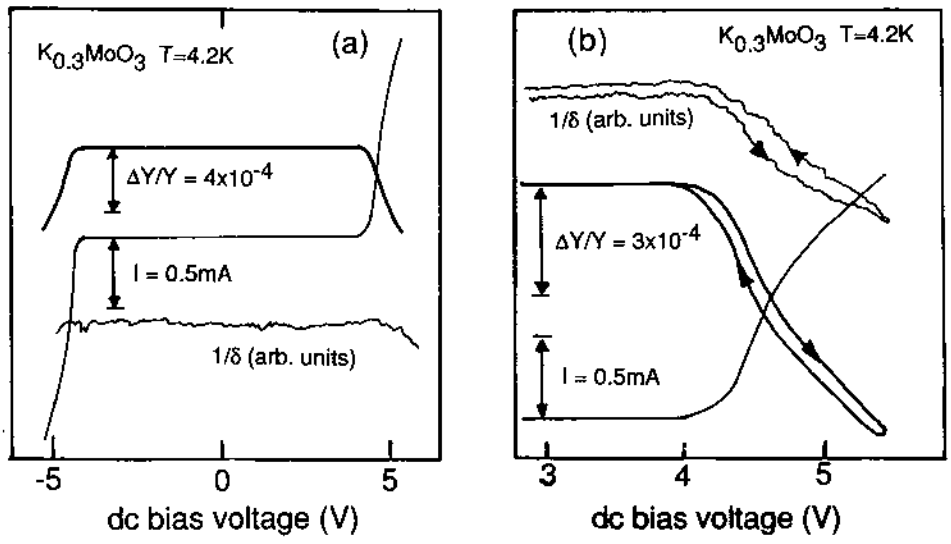

Fig. 4. Bias-dependent electronic and elastic response of $K_{0.3}MoO_3$ at helium temperature. (b) shows the threshold region in detail.

experiments we are not able to rule out heating effects. Heating the sample to above 4K would cause the elastic constants to change in the observed direction. Even if the surface of the sample remained at fixed temperature, the sample core might heat. An independent probe of the core temperature of the sample is needed to correctly interpret our elastic data, as well as the associated electrical conductivity data.

SCANNING TUNNELING MICROSCOPY STUDY OF $K_{0.3}MoO_3$ SURFACE

A scanning tunneling microscope (STM) is a sensitive surface probe, and it has been used successfully to image CDWs in various materials[7,8]. We have attempted to image the CDW in $K_{0.3}MoO_3$ by STM, with the hope of directly observing CDW polarization, domains, and CDW dynamics. Our STM has atomic resolution from 65K to 350K; the temperature is nearly continuously variable. In a related study[8], the microscope has successfully imaged the CDW in 1T-TaS_2 as a function of temperature.

Fig. 5a shows the b-[102] cleavage plane surface of $K_{0.3}MoO_3$ at T=295K, as determined by STM. The bright dots correspond precisely to the expected positions of the K atoms. Fig. 5b shows a similar picture taken in the CDW state at 77K. Again the K atoms are resolved, but unfortunately there is no evidence for additional superlattice structure. A similar result holds true at T=143K and for $Rb_{0.3}MoO_3$ at similar temperatures. The pictures of Fig. 5 are representative of hundreds of pictures recorded (including ones with greater and smaller lateral scale), all with null CDW results. Our results suggest that perhaps the CDW amplitude at the surface of $K_{0.3}MoO_3$ is severly reduced, and is below our present resolution.

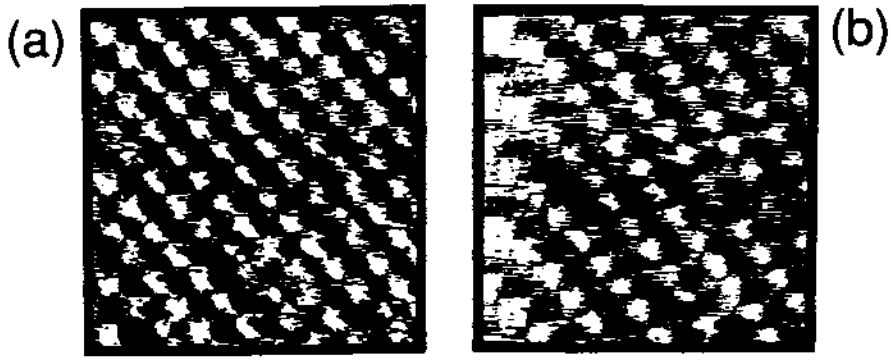

Fig. 5. STM image of $K_{0.3}MoO_3$ surface at (a) 295K and (b) 77K. The nearest neighbor distance between bright spots is approximately 10.5Å.

ACKNOWLEDGEMENTS

This research was supported in part by NSF Grants DMR-8351678 and DMR84-00041 (AZ) and the DOE under contract No. DE-AC03-76SF00098 (JC). UW acknowledges the financial support of the Deutsche Forschungsgemeinschaft DFG, and AZ received support from the Alfred P. Sloan Foundation.

REFERENCES

1 M.F. Hundely and A. Zettl, Solid State Commun. (in press)

2 A. Zettl and G. Grüner, Phys. Rev. B29, 755 (1984)

3 R.J. Cava, R.M. Fleming, P. Littlewood, E.A. Rietman, L.F. Schneemeyer, and R.G. Dunn, Phys. Rev. B30, 3228 (1984)

4 P. Parilla and A. Zettl, Phys. Rev. B32, 8427 (1985), and to be published

5 L.C. Bourne and A. Zettl, Solid State Commun. 60, 789 (1986)

6 L. Mihaly and G.X Tessema, Phys. Rev. B33, 5858 (1986)

7 R.V. Coleman, B. Drake, P.K. Hansma, and G. Slough, Phys. Rev. Lett. 55, 395 (1985)

8 R.E. Thompson, U. Walter, E. Ganz, J. Clarke, A. Zettl, P. Rauch, and F. J. DiSalvo, Phys. Rev. B (submitted)